A PARTICLE SWARM OPTIMIZATION FOR MAXIMUM LOADABILITY AND VOLTAGE/VAR CONTROL

Dissertation submitted in partial fulfillment of the requirements for the award of degree of

Master of Engineering

in

Power Systems & Electric Drives

By:

Priyanka Saini

(Roll. No. 801141019)

Under the supervision of:

Dr. Sanjay K. Jain

Associate Professor, EIED

ELECTRICAL AND INSTRUMENTATION ENGINEERING DEPARTMENT

THAPAR UNIVERSITY

PATIALA – 147004

JULY, 2013

CERTIFICATE

I hereby certify that the work which is being presented in the dissertation entitled, **"A Particle Swarm Optimization for Maximum Loadability and Voltage/VAR Control"**, in partial fulfillment of the requirements for the award of degree of Master of Engineering in Power Systems and Electric Drives submitted in Electrical and Instrumentation Engineering Department of Thapar University, Patiala is an authentic record of my own work carried out under the supervision of Dr. Sanjay K. Jain, Associate Professor, EIED.

The matter presented in this dissertation has not been submitted for the award of any other degree of this or any other university.

Priyanka

(Priyanka Saini)
Roll. No. – 801141019

This is to certify that the above statement made by the candidate is correct and true to best of my knowledge.

Sanjay
13/07/2013

(Dr. Sanjay K. Jain)
Associate Professor
EIED, Thapar University

Countersigned by:

S. Ghosh

(Dr. S. Ghosh)
Professor & Head, EIED
Thapar University

(Dr. S. K. Mohapatra)
Sr. Professor & Dean (Academic Affairs)
Thapar University

ACKNOWLEDGEMENT

I feel honoured in expressing my profound sense of gratitude to Dr. Sanjay K. Jain, Associate Professor, EIED, Thapar University, for his gracious efforts, patient guidance, valuable suggestions and wise counsel for the successful fulfillment of the dissertation work.

I am highly grateful to Dr. S. Ghosh, Professor & Head, EIED, Thapar University, for providing the facilities to carry out the dissertation work.

I would also like to offer my sincere thanks to Ms. Manbir Kaur, Associate Professor & PG Coordinator (Power Systems & Electric Drives), EIED, Thapar University, for her ever supporting and encouraging nature.

I also express my gratitude to entire faculty members of the department for their intellectual support throughout the course of this work.

I am indebted to all whosoever have contributed to carry out this work.

Priyanka

Priyanka Saini

(801141019)

ABSTRACT

As power system networks are becoming highly stressed due to ever-increasing demand, the maximum loadability is achieving great importance. The maximum loadability is also related to voltage stability and security assessment. In this work, Particle Swarm Optimization (PSO) is presented to obtain maximum loadability. The problem to obtain maximum loadability is expressed as an optimization problem. The maximum loadability at a given bus is obtained by taking real load demand at that bus as variable. The load power factor is maintained corresponding to base case power factor at that bus or to specified value. The maximum loadabilities are obtained for various standard systems namely, 2-Bus, 4-Bus, 6-Bus and 14-Bus system and the obtained results from developed PSO based algorithm are compared with Continuation Power Flow (CPF), a widely accepted exact method. The Voltage/VAR control problem has been attempted using PSO by minimizing the real power losses. Both the continuous (automatic voltage regulation supported PV bus voltages) and the discrete variables (on-load tap changer transformers and shunt capacitors) are used as state variables in voltage/VAR control. The voltage/VAR control problem is solved for various systems namely, 4-Bus, 6-Bus and 14-Bus system.

TABLE OF CONTENTS

LIST OF FIGURES

LIST OF TABLES

CHAPTER-1

INTRODUCTION

1.1 OVERVIEW

Voltage stability is an important aspect as power system is becoming heavily loaded or stressed day-by-day due to increase in power demand [1]. The stress on the system can be reduced by expansion of the system. However, expansion of the system is limited due to the constraints imposed by environment and economy. Restructuring of the electrical power system has brought voltage stability to the main focus. Voltage stability is concerned with the ability of a power system to maintain acceptable voltages at all buses in the system under normal conditions and after being subjected to a disturbance [2]. It is due to the failure of system to meet needed reactive demand. Voltage instability may lead to voltage collapse. Many voltage collapse incidents have been reported [3]. Thus it is a fundamental concern in the planning and operation of power system.

There are many reasons for voltage instability. One of them is the increase in load demand. The increase in load demand results in reduced stability margin. The stability margin or load margin is the difference between the current operating point and maximum loading point of the system. The methods to find the load margin include sensitivity analysis [4], modal analysis [5], interior point optimization method [6] etc. The conventional power flow techniques suffer from divergence near the critical point due to mathematical limitations.

The continuation power flow (CPF) is an extensively used method to find the maximum loadability which uses continuation parameterization technique, corrector and predictor steps to draw a P-V curve for a particular bus in the system [7-8]. It overcomes the problem of divergence near the critical point (maximum loadability, corresponding voltage) by using parameterization technique. The critical point is then used to find the load margin. But the CPF involves complex mathematical formulations.

In this work, particle swarm optimization (PSO), an evolutionary computation technique [9] has been used to search for the critical point without drawing P-V curve. It is a

heuristics-based swarm intelligence method [10]. The particle swarm optimization has also been used to handle both continuous and discrete variables in voltage/VAR control by minimizing the real power losses.

1.2 LITERATURE REVIEW

Cutsem [1] has explained the phenomena of voltage instability, its countermeasures and analysis methods. He has discussed the threats posed by voltage instability that it may take form of a dramatic drop of transmission system voltages which may lead to total system disruption. The countermeasures and analysis methods have also been elaborated.

Atputharajah *et al*. [3] have reported literatures on power system stability, reliability and several major blackouts. They have commented on root causes, lessons learnt from the blackouts and solutions.

Begovic and Phadke [4] have used minimum singular value of the Jacobian matrix and total generated reactive power as indicators of stability margin for a class of voltage instabilities which correspond to static bifurcations of load flow equations and sensitivity methods for reactive support allocation.

Gao *et al*. [5] have discussed voltage stability analysis of large power systems using a modal analysis technique. They have used a steady state system model to compute a specified number of smallest eigen values and the corresponding eigen vectors of a reduced Jacobian matrix. Each eigen value is associated with a mode of voltage/reactive variation providing a relative measure of proximity to voltage instability.

Irisarri *et al*. [6] have proposed a non-linear optimization interior point (IP) method for the determination of maximum loadability in a power system. They have presented pure primal-dual and predictor-corrector primal-dual IP algorithms.

Mallick *et al*. [11] have presented three schemes using fuzzy logic (FL) along with a new formation of sparse constant array to find the maximum loadability. The iterative process can be started with random initialization using proposed FL schemes. The results are compared with the N-R method technique and the standard fuzzy logic controllers.

Ajjarapu and Christy [7] have presented a method of finding a continuum of power flow solutions starting at some base load and leading to the steady state voltage stability limit

(critical point) of the system. It remains well-conditioned at and around the critical point.

Chiang *et al*. [8] have also presented the CPF for tracing power system steady-state stationary behavior due to parameter variations. The variations include general bus real and/or reactive loads, area real and/or reactive loads, or system-wide real and/or reactive loads, and real generation at P-V buses.

Kennedy and Eberhart [9] have introduced a method for optimization of continuous nonlinear functions. They have described the PSO concept in terms of its precursors, briefly reviewing the stages of its development from social simulation to optimizer.

Valle *et al*. [10] have presented a detailed overview of the basic concepts of PSO and its variants. They have also provided a comprehensive survey on the power system applications that have benefited from the powerful nature of the PSO as an optimization technique. For each application, technical details that are required for applying PSO, such as its type, particle formulation (solution representation), and the most efficient fitness functions are also discussed.

AlRashidi and El-Hawary [12] have presented a comprehensive coverage of different PSO applications in solving optimization problems in the area of electric power systems. They have also explored recent trends with regard to PSO development in this area. The possible future applications of PSO in the area of electric power systems and its potential theoretical studies are also discussed.

Acharjee [13] has developed simple real coded security constraint genetic algorithm (SCGA) to solve the problem of maximum loadability limit (MLL). If MLL is identified, load margin, voltage stability, security margin can be determined and precaution can be taken.

Gnanambal and Babulal [14] have presented an algorithm to determine the maximum loadability limit of power system using hybridization of differential evolution (DE) and PSO (DEPSO) to incorporate the advantages of both methods. They have compared the performance of this DEPSO algorithm with other evolutionary algorithms like DE and multi agent hybrid PSO and statistical measures.

El-Dib *et al*. [15] have also presented that maximum loading point can be formulated as an optimization problem. They have utilized the newly developed evolutionary PSO in

solving this optimization problem. The results are compared to those obtained by the widely used CPF technique.

Arya *et al*. [16] have used co-ordinated aggregation based PSO (CAPSO) as optimization technique for rescheduling reactive power control variables so as to have an adequate loadability margin for current operating point. Two objective functions have been selected for load margin enhancement. One is minimization of total reactive power loss and other considers minimization of incremental reactive power loss.

Shunmugalatha and Slochanal [17] have utilized the newly developed multiagent-based hybrid particle swarm optimization (MAHPSO) method for solving the problem of maximum loadability limit of power systems, one of the approaches to voltage stability. MAHPSO is a combination of genetic algorithm (GA), PSO, and multi agent system (MAS). Multiagent-based hybrid particle swarm optimization combines both the features of MAPSO and HPSO.

Shunmugalatha and Slochanal [18] have also presented formulation of optimum cost of generation for maximum loadability limit of power system as an optimization problem, which consists of two steps namely computing maximum loadability limit and the optimum cost of generation for maximum loadability limit. They have utilized the hybrid PSO, which incorporates the breeding and subpopulation process in GA into PSO.

Selvi and Gnanambal [19] have used DE to determine voltage stability. Althowibi and Mustafa [20] have discussed sensitivity and modal analysis for the same.

Yoshida *et al*. [21] have presented a PSO for voltage/VAR Control considering voltage security assessment (VSA). Voltage/VAR can be formulated as mixed-integer nonlinear optimization problem (MINLP). The original PSO has been expanded to handle a MINLP and determine an on-line VVC strategy with continuous and discrete control variables such as automatic voltage regulator (AVR) operating values of generators, tap positions of on-load tap changer (OLTC) of transformers, and the number of reactive power compensation equipments.

Tomsovic [22] has modeled multiple objectives and soft constraints of practical voltage control problem using fuzzy sets. Piece-wise linear convex membership functions for the fuzzy sets are defined. Under this definition, the fuzzy optimization problem is reformulated as a standard linear programming problem.

Ramos *et al*. [23] have developed a hybrid tool to assist the operator in voltage/VAR control and optimization. Advantage is taken of both numerical (conventional) and heuristic (knowledge-based) methods in order to find a practical number of control variables (smooth and/or discrete) which can be used to solve voltage violations or to reduce power losses.

Cheng *et al*. [24] have presented a methodology called sensitivity tree for control of voltage/VAR. Swarup and Subash [25] have proposed a neural-network based solution for the same. Wu *et al*. [26] have applied improved PSO to the voltage/VAR control. Liu *et al*. [27] have presented multi-objective adaptive particle swarm optimization (MOAPSO) for the problem. Liang and Wang [28] have given a fuzzy-based approach to control voltage/VAR in the distribution system. Vlachogiannis and Lee [29] have introduced coordinated aggregation particle swarm optimization (CAPSO) to solve the problem.

1.3 OBJECTIVES OF THE WORK

The work is carried out with the objective to obtain the maximum loadability using PSO based optimization algorithm and compare its effectiveness with the existing known algorithm. The work is also carried out to find the setting of continuous and discrete variables for voltage/VAR control by minimizing the losses.

1.4 ORGANIZATION OF THE DISSERTATION

The dissertation has been organized into five chapters. The chapter 1 includes overview, literature review, objectives of the work and organization of the dissertation. The Chapter 2 briefly defines voltage stability and describes CPF. The Chapter 3 discusses PSO, its application to find maximum loadability, corresponding algorithm and flowchart and obtained results. The results obtained using PSO based algorithm are also compared with the CPF. The Chapter 4 highlights the state variables used to control voltage and VAR. The formulated problem, algorithm, flowchart and results have also been discussed. The Chapter 5 summarizes the conclusions and future scope of work.

CHAPTER-2

VOLTAGE STABILITY AND CONTINUATION POWER FLOW

This chapter reviews the definitions and classifications of voltage stability. There are many reasons for voltage instability. The increase in load is one of them. The CPF is a well-known method to find the critical load beyond which system becomes unstable. Thus CPF has been discussed.

2.1 VOLTAGE STABILITY

IEEE/CIGRE joint task force on stability terms and definitions defined power system stability [34]. The task force also classified power system stability as rotor angle stability, frequency stability, and voltage stability. In general voltage stability is concerned with the ability of a power system to maintain acceptable voltages at all buses in the system under normal conditions and after being subjected to a disturbance [2]. Voltage stability includes large disturbance voltage stability, small disturbance voltage stability, short-term voltage stability and long-term voltage stability. These are described as follows [31]:

A) Large-Disturbance Voltage Stability

It refers to the system's ability to maintain steady voltages following large disturbances such as system faults, loss of generation, or circuit contingencies. This ability is determined by the system and load characteristics, and the interaction of both continuous and discrete controls and protections. The study period of interest may extend from a few seconds to tens of minutes.

B) Small-Disturbance Voltage Stability

It refers to the system's ability to maintain steady voltages when subjected to small perturbations such as incremental changes in system load. This form of stability is influenced by the characteristics of loads, continuous controls, and discrete controls at a given instant of time.

C) Short-Term Voltage Stability

It involves dynamics of fast acting load components such as induction motors, electronically controlled loads and HVDC converters. The study period of interest is in the order of several seconds, and analysis requires solution of appropriate system differential equations.

D) Long-Term voltage stability

It involves slower acting equipment such as tap-changing transformers, thermostatically controlled loads and generator current limiters. The study period of interest may extend to several or many minutes, and long-term simulations are required for analysis of system dynamic performances. Instability is due to the loss of long-term equilibrium, post-disturbance steady-state operating point being small-disturbance unstable, or a lack of attraction towards the stable post-disturbance equilibrium. The disturbance could also be a sustained load build up.

Thus voltage stability is influenced by characteristics of generators, loads and reactive power compensation devices.

2.2 CRITICAL VOLTAGE AND MAXIMUM POWER

Consider the system in Fig. 2.1. The voltage at receiving end changes with the variation in load power. The graph depicting the variation of load bus voltage with demand power is known as P-V curve. The increase in load at the given bus results in decrease of voltage at that bus. There is certain maximum power at which voltage becomes critical. Thus maximum power transfer relates voltage instability [31].

The voltage at the receiving end is given by equation (2.1).

$$\vec{V}_R = \vec{V}_S - jX\vec{I}_L \tag{2.1}$$

Then the line current is given by equation (2.2)

$$\vec{I}_L = \frac{\vec{V}_S - \vec{V}_R}{jX} \tag{2.2}$$

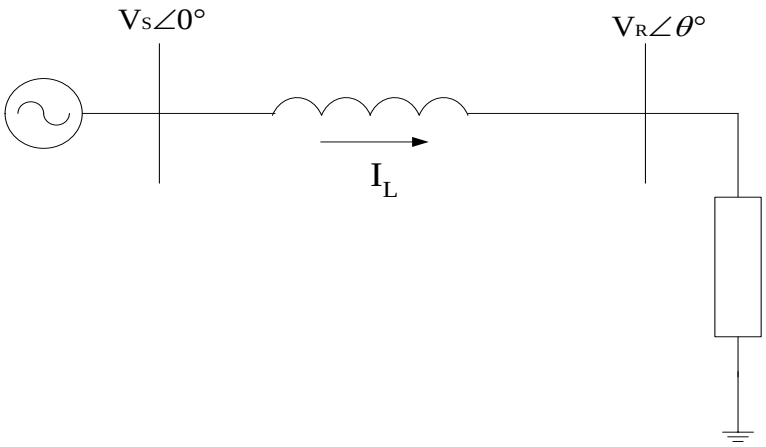

Fig. 2.1 A generator connected to a load

The complex power is given as in following equations.

$$S = V_R I_L^* \tag{2.3}$$

$$S = V_R \left(\frac{\vec{V}_S - \vec{V}_R}{jX} \right)^* \tag{2.4}$$

$$= \vec{V}_R \left(\frac{\vec{V}_S^* - \vec{V}_R^*}{-jX} \right) \tag{2.5}$$

$$= V_R \angle \Theta \left(\frac{V_S \angle 0 - V_R \angle -\Theta}{-jX} \right) \tag{2.6}$$

$$= -\frac{V_S V_R}{X} sin\Theta + j\left(\frac{V_S V_R}{X} cos\Theta - \frac{V_R^2}{X} \right) \tag{2.7}$$

The complex power can be separated into real and imaginary parts which correspond to real and reactive power as shown in equations (2.9) and (2.10).

$$S = P + jQ \tag{2.8}$$

$$P = -\frac{V_S V_R}{X} sin\Theta \tag{2.9}$$

$$Q = \frac{V_S V_R}{X} cos\Theta - \frac{V_R^2}{X} \tag{2.10}$$

From equations (2.9) and (2.10) values of sinΘ and cosΘ are substituted in equation (2.11).

$$sin^2\Theta + cos^2\Theta = 1 \tag{2.11}$$

$$\left(\frac{-PX}{V_S V_R}\right)^2 + \left(\frac{QX + V_R^2}{V_S V_R}\right)^2 = 1 \tag{2.12}$$

Solving equation (2.12), we have equation (2.13).

$$\frac{V_R^4}{V_S^4} + \frac{V_R^2}{V_S^4}(2QX - V_S^2) + \frac{X^2}{V_S^4}(P^2 + Q^2) = 0 \tag{2.13}$$

Let σ be the power factor angle of the load and then Q is given by equation (2.14).

$$Q = P\,tan\sigma \tag{2.14}$$

Put equation (2.14) in equation (2.13).

$$\frac{V_R^4}{V_S^4} + \frac{V_R^2}{V_S^4}(2XP\,tan\sigma - V_S^2) + \frac{X^2}{V_S^4}(P^2 + P^2\,tan^2\sigma) = 0 \tag{2.15}$$

Rearranging and solving equation (2.15), we have equation (2.18).

$$\frac{V_R^4}{V_S^4} + \frac{V_R^2}{V_S^4}(2XP\,tan\sigma - V_S^2) + \frac{X^2P^2}{V_S^4}(sec^2\sigma) = 0 \tag{2.16}$$

$$\frac{V_R^4}{V_S^4} + \frac{V_R^2}{V_S^2}\left(\frac{2XP\,tan\sigma}{V_S^2} - 1\right) + \frac{X^2P^2}{V_S^4}(sec^2\sigma) = 0 \tag{2.17}$$

$$\frac{V_R^2}{V_S^2} = -\left(\frac{2XP\,tan\sigma}{V_S^2} - 1\right) \pm \frac{\sqrt{\left(\frac{2XP\,tan\sigma}{V_S^2} - 1\right)^2 - 4\frac{X^2P^2}{V_S^4}\,sec^2\sigma}}{2} \tag{2.18}$$

Equation (2.18) has four solutions. Two solutions from them are physically meaningful which correspond to high voltage and low voltage solution. These solutions are shown in Fig. 2.2.

There is a point where only one solution exists and this is known as critical point. The critical point corresponds to maximum power point and critical voltage. At this point the term

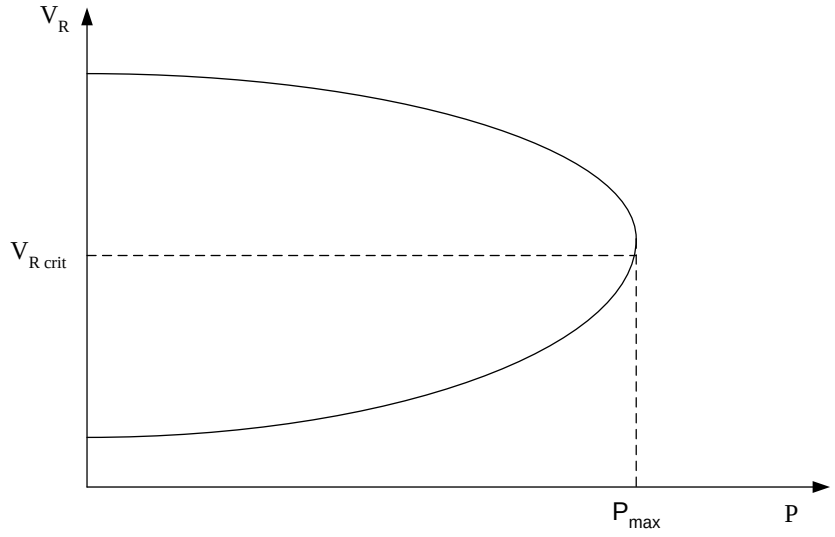

Fig. 2.2 The variation of voltage at load bus w.r.t power

inside the square root becomes zero. Using this, maximum power and critical voltage at load bus is determined.

$$P_{max} = \frac{{V_S}^2 cos\sigma}{2X(1 + sin\sigma)} \tag{2.19}$$

$$V_{R\,crit} = \frac{V_S}{\sqrt{2} * \sqrt{1 + sin\sigma}} \tag{2.20}$$

2.3 CONTINUATION POWER FLOW

The increase in load at load bus results in decrease in voltage at that bus and beyond a point known as critical point system loses equilibrium. The power transferred corresponding to the critical point is the maximum power which can be transferred. This maximum power relates to the voltage instability for constant power loads.

One can draw P-V curve for particular load bus by using power flow equations and Jacobian matrix for the system. But the Jacobian becomes singular at the maximum power point and thus conventional methods fail to converge at this point. For avoiding this problem

there are many computational techniques based on bifurcation and continuation methods. The CPF is one of them.

The CPF is based on continuation methods. The continuation method is mathematical path-following methodology. Continuation methods consist of predictor, corrector, step length control, parameterization strategy and so is the CPF. It is used to solve system of non linear equations. It can find solution near the critical point easily. For this, it uses local parameterization continuation technique [7, 8].

Consider power flow equations (2.21) at load bus 2 in two bus system in Fig. 2.3.

$$P\ (V, \delta) = 0$$
$$Q\ (V, \delta) = 0 \qquad (2.21)$$

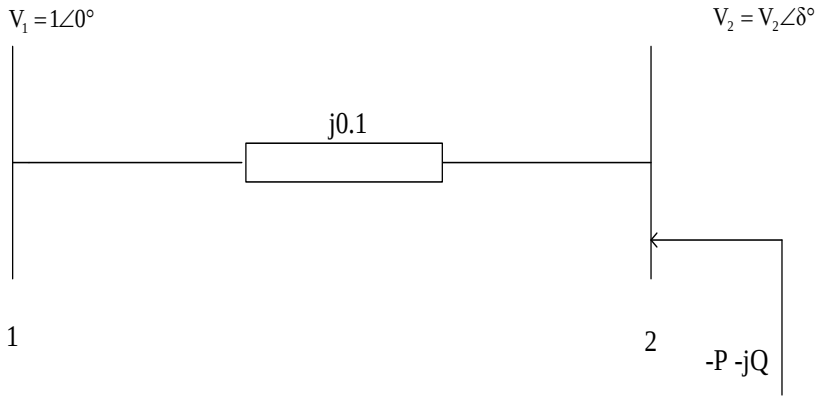

Fig. 2.3 Two bus system

These equations (2.21) are added with a load parameter, λ. Thus equations (2.21) are modified to equations (2.22).

$$P\ (V, \delta, \lambda) = 0$$
$$Q\ (V, \delta, \lambda) = 0 \qquad (2.22)$$

where load change scenarios are incorporated in P and Q as in equations (2.23).

$$P = P_0 * (1 + \lambda K)$$
$$Q = Q_0 * (1 + \lambda K) \qquad (2.23)$$

$$Q_0 = P_0 * tan(\psi) \tag{2.24}$$

where

P_0 = original real power of load

Q_0 = original reactive power of load

K = rate of change of load

Ψ = power factor angle of load

Original Jacobian matrix for this system is given by equation (2.25).

$$J_0' = \begin{bmatrix} \frac{\partial P}{\partial \delta} & \frac{\partial P}{\partial V_2} \\ \frac{\partial Q}{\partial \delta} & \frac{\partial Q}{\partial V_2} \end{bmatrix} \tag{2.25}$$

The Jacobian is augmented by one column. The augmented Jacobian is given as in equation (2.26).

$$J_0 = \begin{bmatrix} \frac{\partial P}{\partial \delta} & \frac{\partial P}{\partial V_2} & \frac{\partial P}{\partial \lambda} \\ \frac{\partial Q}{\partial \delta} & \frac{\partial Q}{\partial V_2} & \frac{\partial Q}{\partial \lambda} \end{bmatrix} \tag{2.26}$$

A row vector, e with all elements equal to zero except one element chosen properly which is equal to one, is appended to augmented Jacobian to normalize the tangent vector, t. The tangent vector is the vector of differentials. The value of one of the variable is mentioned as either +1 or -1. This particular variable is the continuation parameter as shown in equation (2.27).

$$\begin{bmatrix} J_0 \\ e \end{bmatrix} * t = \begin{bmatrix} 0 \\ \pm 1 \end{bmatrix} \tag{2.27}$$

Tangent vector,

$$t = [d\delta \; dV_2 \; d\lambda]^T \tag{2.28}$$

The tangent vector is found using equation (2.27) and prediction is made using equation (2.29).

$$\begin{bmatrix} \delta^{n+1} \\ V_2^{n+1} \\ \lambda^{n+1} \end{bmatrix} = \begin{bmatrix} \delta^{n} \\ V_2^{n} \\ \lambda^{n} \end{bmatrix} + \sigma \begin{bmatrix} d\delta \\ dV_2 \\ d\lambda \end{bmatrix} \tag{2.29}$$

where n is the number of iteration, σ is the specified step length. The σ is modified in subsequent iterations according to the equation (2.30)

$$\sigma_{new} = \sigma_{old} \, N_{opt} / N_j \tag{2.30}$$

where

N_{opt} = optimal number of corrector iterations

N_j = number of iterations required to correct the previous predicted solution

And then newton raphson method is used to correct the predicted value.

For a particular maximum value of the continuation parameter chosen, λ, solution doesn't exist. At this time continuation parameter is changed. Now, one of the state variables is chosen as continuation parameter. That's why this is known as locally parameterized continuation. One way to select continuation parameter correctly is to start from λ and then after each iteration the state variable with largest tangent vector is chosen as continuation parameter.

For stopping criteria it has to find out that whether the critical point has been reached or not. This information can be collected from the sign of tangent component corresponding to λ, dλ. It becomes negative once it passes the critical point. One may also use P-V curve slopes for assessing the critical point.

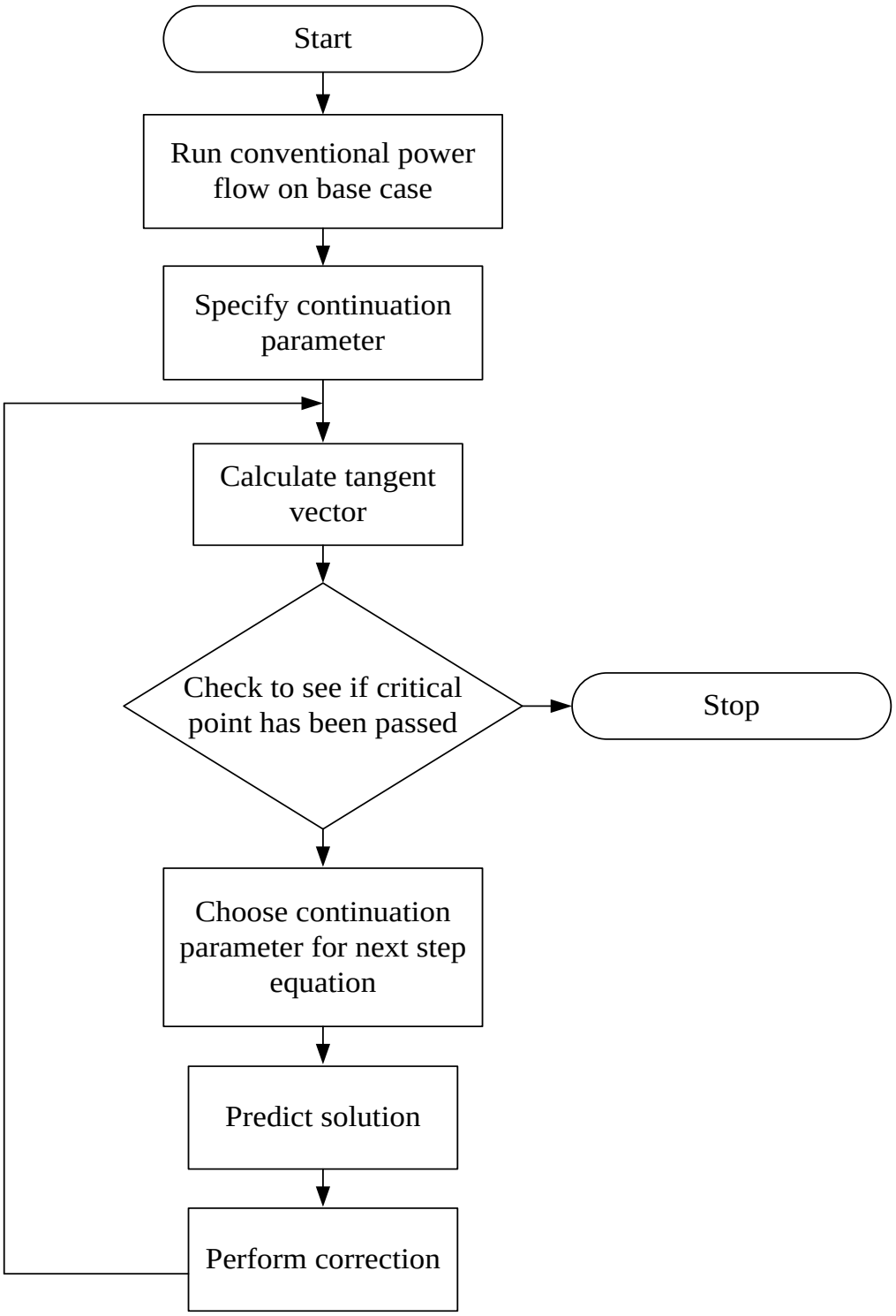

Fig. 2.4 A flowchart of the CPF

Thus CPF overcomes the problem of not converging at critical point by using continuation parameter technique. The flowchart of the CPF has been depicted in Fig.2.4 [7].

CHAPTER-3

MAXIMUM LOADABILITY USING PARTICLE SWARM OPTIMIZATION

This Chapter first reviews the basics of PSO, an evolutionary computation technique and then the problem of maximum loadability is been formulated using PSO wherein different variables and algorithm used are discussed. The obtained results using PSO based algorithm for maximum loadability and its comparison to CPF are given in the chapter.

3.1 PARTICLE SWARM OPTIMIZATION

The PSO is based on the behaviour of different organisms for example, school of fish and flock of bird. It provides a search procedure based on population. Every Particle (individual) modifies its position in multi-dimensional space according to its own and neighbours' experience. The best position of each particle is saved as the local best position and the best position among all these is recorded as the global best position [9-10]. Vel denotes the velocity of each particle. The modified velocity and position of each particle is given by equation (3.1) and (3.2).

$$Vel_{ij}^{n+1} = C_1 * Vel_{ij}^{n} + C_2 * rand * \left(lbest_{ij}^{n} - P_{ij}^{n}\right) + C_3 * rand * \left(gbest_{j}^{n} - P_{ij}^{n}\right) \quad (3.1)$$

$$P_{ij}^{n+1} = P_{ij}^{n} + Vel_{ij}^{n+1} \quad (3.2)$$

for (i = 1,2…..s, j = 1,2 ……m)

where

s = number of particles in a group

m = number of members in a particle

C_1 = inertia weight factor

C_2 and C_3 = acceleration constants

rand = uniform random values

Vel_{ij}^{n} = velocity of j^{th} member of i^{th} particle at n^{th} iteration

P_{ij}^{n} = current position of j^{th} member of i^{th} particle at n^{th} iteration

$lbest_{ij}^{n}$ = local best value of j^{th} member of i^{th} particle at n^{th} iteration

$gbest_{j}^{n}$ = global best value of j^{th} member at n^{th} iteration

Velocity should not be too slow or too high to avoid exploring not beyond local solution and avoid bypassing good solutions respectively. Thus velocity of each particle should lie between a particular minimum and maximum value of velocity. Constants C_2 and C_3 make each particle to achieve local best and global best positions. These are set equal to 2 according to past experiences. The inertia weight is set according to the following equation (3.3).

$$C_1 = C_1^{max} - \left(\frac{C_1^{max} - C_1^{min}}{IT^{max}} * IT\right) \quad (3.3)$$

where

IT^{max} = maximum no. of iterations

IT = current number of iteration

3.2 PROBLEM FORMULATION

The critical point (maximum real power demand, and the corresponding voltage), has been evaluated by simulating the problem as an optimization problem. It is formulated as shown in equation (3.4).

$$Minimize \ \frac{1}{1 + (V_i - 1)^2 + (Pd_i)^2} \quad (3.4)$$

where

Pd_i = real power demand at the load bus i

V_i = corresponding voltage at the load bus i

i = load bus

subject to the

(i) Equality constraint

$$P_{gk} = P_{dk} + P_k \quad (3.5)$$

for (k = 1,2,……no. of buses)

where,

P_{gk} = real power generation at k^{th} bus

P_{dk} = real power demand at k^{th} bus

P_k = injected real power at k^{th} bus

The load flow normally considers inequality constraints for voltages at PQ buses and reactive power at PV buses. However, for computation of maximum loadability, these inequality constraints are not considered.

3.2.1 STATE VARIABLES

Real power demand is varied at the load bus i for which critical point is to be located. It is varied between a minimum and maximum value. Minimum value is taken as zero. Maximum value can be taken as suitably a high value number, say, 20 or 30 per unit.

Ratio of reactive power and real power demand of i^{th} bus of base case data is determined. Reactive power is then varied in the same ratio to maintain the power factor constant.

3.2.2 ALGORITHM

The PSO has been used to find the maximum loadability. The search procedure for the critical point has been outlined below:

Step 1. Read the essential data.

Step 2. Velocities and initial set of solution of real power demand are generated randomly within their respective limits. The reactive power demand is computed keeping load power factor as constant.

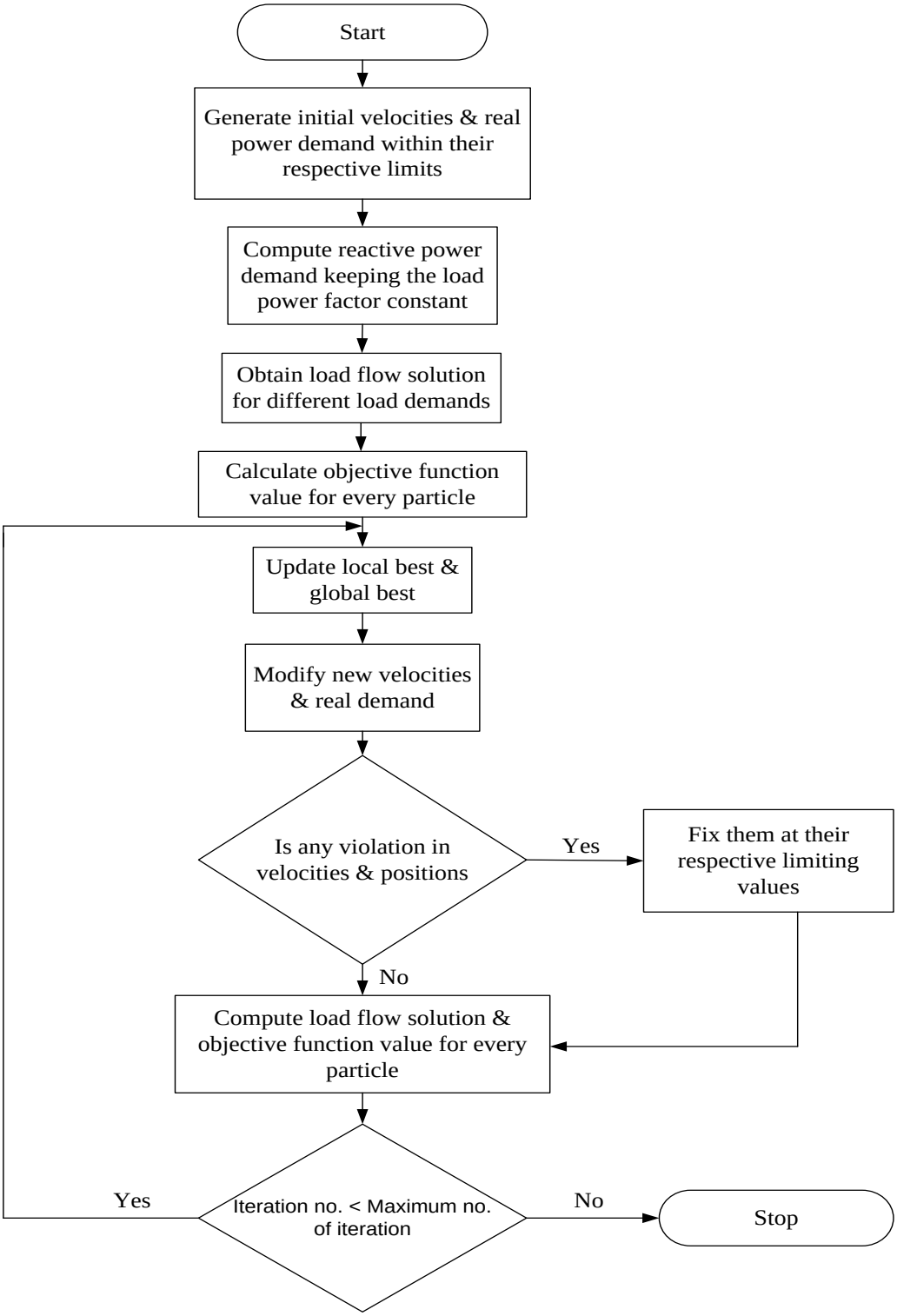

Fig. 3.1. A flowchart to obtain maximum loadability using PSO based algorithm

Step 3. The bus data is modified according to the population generated. And then the load flow solution is modified.

Step 4. The objective function values are calculated using equation (3.4) for every particle of population.

Step 5. Update the local best and the global best with the consideration of objective function values.

Step 6. Modify the new velocities using the local best and global best using equation (3.1). Also calculate the real load demand using equation (3.2) and compute reactive load demand for keeping power factor constant.

Step 7. If any violation in velocities and load demand, updated position, they are fixed at their respective limiting values.

Step 8. Compute load flow solution for new position, objective function value for each particle.

Step 9. If iteration no. is greater than the maximum no. of iteration then stop, otherwise go to step 5.

A flowchart of PSO to obtain maximum loadability has been depicted in Fig. 3.1.

3.3 RESULTS AND DISCUSSION

The developed algorithm based on PSO to obtain maximum loadabilty is carried out on different power systems namely 2-Bus, 4-Bus, 6-Bus and IEEE 14- Bus system. The data of these test systems is given in Table A1, A2, A3 and A4 respectively. The results obtained from the PSO are compared with the CPF.

3.3.1 CASE 1

The study is carried on 2-Bus test system with one slack and one load bus. To understand the dependency of maximum loadability with load power factor, the analysis is carried out for load power factors as 0.8 lagging, unity and 0.8 leading. The maximum loadability as obtained from PSO and CPF are summarized in Table 3.1. The corresponding

voltages at maximum loadability are tabulated in Table 3.2. The P-V curve obtained from the CPF is also shown in Fig. 3.2 for unity power factor load.

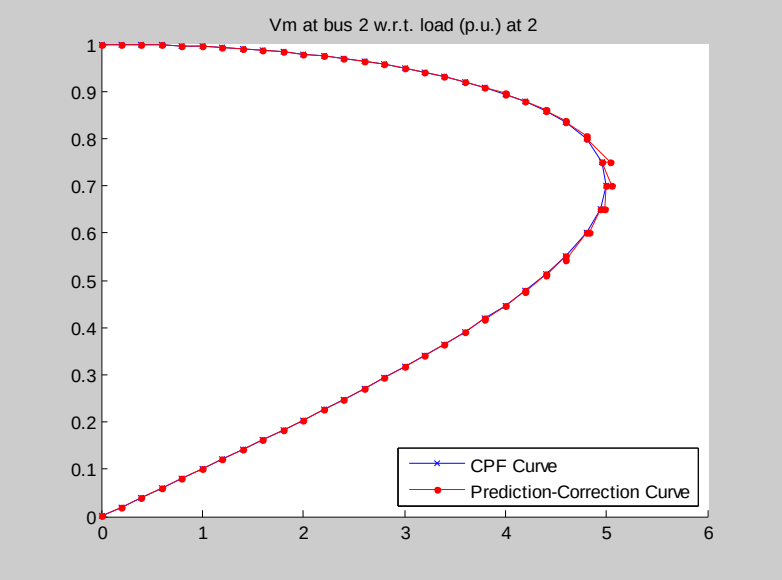

Fig. 3.2. The variation of bus 2 voltages with load (2-Bus system)

As evident from Table 3.1, the maximum loadability for 0.8 leading power factor load is maximum (9.9883) whereas it is minimum for 0.8 lagging power factor (2.4706). This demonstrates that higher load can be supplied for leading power factor load. The results obtained from developed PSO based algorithm are found comparable with CPF. The CPF, a derivative based arrangement, is able to calculate the nose point and therefore the loadability is slightly higher due to CPF and so the bus voltage is slightly lower by CPF.

Table 3.1. The maximum loadability of load bus 2 varied with different power factors (2-Bus system)

Power Factor	**CPF**	**PSO**
	Load Bus 2 Varied	
0.8 Lagging	2.4999	2.4706
Unity	4.9990	4.9972
0.8 Leading	9.9942	9.9883

Table 3.2. The corresponding voltages at the maximum loadability point at different power factors (2-Bus system)

Bus	Power Factor					
	0.8 Lagging		**Unity**		**0.8 Leading**	
	CPF	**PSO**	**CPF**	**PSO**	**CPF**	**PSO**
1	1.0	1.0	1.0	1.0	1.0	1.0
2	0.5567	0.6125	0.7000	0.7187	1.1297	1.1346

3.3.2 CASE 2

The proposed method is studied for 4-Bus data which consists of one slack, one generator and two load buses. The load at second and third load bus is varied one by one to obtain maximum loadability for respective buses. The obtained results of maximum loadability at second and third bus using PSO based algorithm and CPF are summarized in Table 3.3, the load power factor as mentioned by base case data is kept unchanged. The P-V curve obtained for third load bus, for base case load power factor (0.85 lagging) from CPF is depicted in Fig. 3.3.

Table 3.3. The maximum loadability at different varied load buses (4-Bus system)

Case System	Load Bus	Maximum Loadability	
		CPF	**PSO**
4 – Bus	**3**	10.600	10.586
	2	11.2587	11.256

For third bus, the analysis is also carried out with load power factors as 0.8 lagging, unity and 0.8 leading. The maximum loadability obtained from developed PSO and CPF with different power factors at third bus is given in Table 3.4. The results verify that maximum loadability of 0.8 lagging (9.637), unity (17.080) and 0.8 leading power factor (26.595) is in the increasing order.

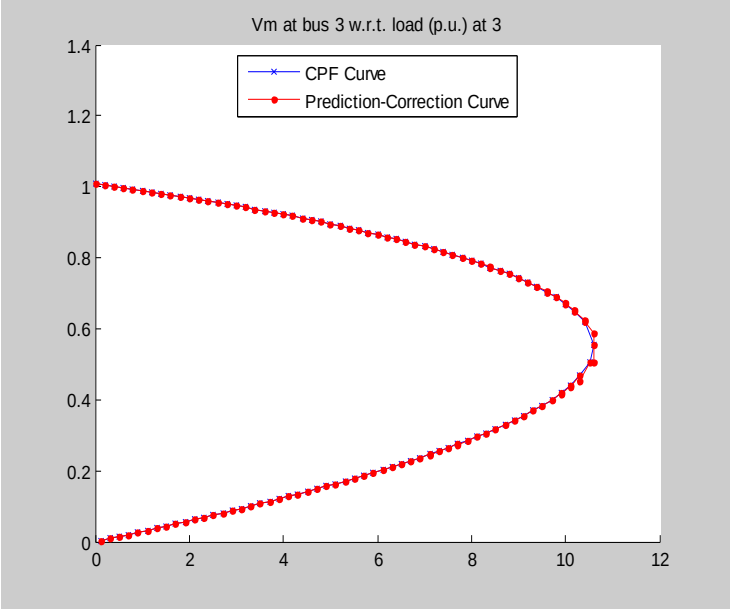

Fig. 3.3. The variation of bus 3 voltages with load (4-Bus system)

Table 3.4. The maximum loadability of load bus 3 varied with different power factors (4-Bus system)

Power Factor	**CPF**	**PSO**
	Load Bus 3 Varied	
0.8 Lagging	9.6377	9.637
Unity	17.0804	17.080
0.8 Leading	26.6000	26.595

3.3.3 CASE 3

The maximum loadability is obtained using developed PSO for different load buses of 6-Bus data. 6-Bus data consists of two generator, three load and one slack bus. The load at sixth, fifth and fourth load bus is varied. The load at one load bus is varied at a time. The maximum loadability obtained from developed PSO and CPF for different load buses is given in the Table 3.5. The P-V curve for sixth load bus obtained from CPF for 0.7071 lagging power factor load is depicted in Fig. 3.4.

The fifth load bus is tested for different power factors, 0.8 leading, unity and 0.8 lagging. The maximum loadability at fifth bus for these power factors is summarized in Table 3.6. It is again demonstrated from the maximum loadability results of 0.8 lagging (3.2122), unity (5.0406) and 0.8 leading power factor (6.3831) load that higher load can be supplied for leading power factor load.

Table 3.5. The maximum loadability at different varied load buses (6-Bus system)

Case System	Load Bus	Maximum Loadability	
		CPF	**PSO**
6 – Bus	**6**	3.3867	3.3755
	5	2.7920	2.7557
	4	3.0894	3.0732

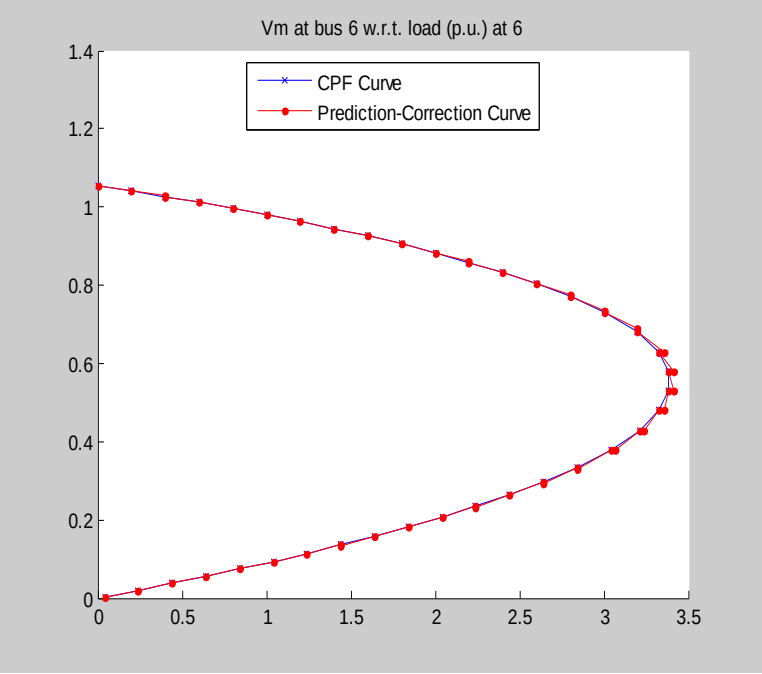

Fig. 3.4. The variation of bus 6 voltages with load (6-Bus system)

Table 3.6. The maximum loadability of load bus 5 varied with different power factors (6-Bus system)

Power Factor	**CPF**	**PSO**
	Load Bus 5 Varied	
0.8 Lagging	3.2391	3.2122
Unity	5.0653	5.0406
0.8 Leading	6.3845	6.3831

3.3.4 CASE 4

The proposed method is also tested for 12th bus of IEEE 14-Bus test system. The obtained results of maximum loadability using PSO based algorithm are summarized in Table 3.7, which are found comparable with CPF. For leading power factor load maximum loadability is greatest (2.6704). The loadability obtained from CPF is slightly higher as it is a derivative based method to find the critical point.

Table 3.7. The maximum loadability of load bus 12 varied with different power factors (14-Bus system)

Power Factor	**CPF**	**PSO**
	Load Bus 12 Varied	
0.8 Lagging	1.3655	1.3492
Unity	2.1297	2.1
0.8 Leading	2.6726	2.6704
As per the base case data	1.8372	1.8238

CHAPTER-4

VOLTAGE/VAR CONTROL

In this chapter the voltage/VAR control problem has been attempted using PSO by minimizing the real power losses. Both the continuous (automatic voltage regulation, AVR) and discrete variables (on-load tap changer transformers and shunt capacitors) have been used as state variables in voltage/VAR problem. The modelling of regulating transformer is also discussed. The voltage/VAR problem formulation with the various constraints, algorithm and flowchart is discussed.

4.1 STATE VARIABLES

Both the continuous and discrete variables are used as state variables in the voltage/VAR control problem [21]. The continuous variables include AVR whereas discrete variables consist of on-load tap changer transformers and shunt capacitors.

4.1.1 AUTOMATIC VOLTAGE REGULATION

The percentage voltage regulation is defined as:

$$\frac{V_t(no-load) - V_t(rated)}{V_t(rated)} * 100\% \qquad (4.1)$$

where

V_t (rated) = the terminal voltage at the full-load and specified power factor

V_t (no-load) = the terminal voltage at no-load keeping the field current constant as it is at the full load and specified power factor

Due to the armature reactance and armature reaction, the terminal voltage of the alternator is subjected to change when load current and load power factor is varied. The automatic voltage regulator is used to maintain this voltage constant by changing the field current of the alternator. If the terminal voltage decreases, it increases the field current and

hence the field flux and thus the induced voltage increases. If the terminal voltage increases, it decreases the induced voltage by decreasing the field current.

Automatic voltage regulator is taken as a continuous variable in the PSO based algorithm used for voltage/VAR control problem. It is treated as voltage specification values at P-V buses. The initial values of voltages at PV buses are generated randomly between the maximum and minimum limits of voltages. During the optimization procedure using PSO, voltages are modified between these limits only.

4.1.2 ON-LOAD TAP CHANGER OF TRANSFORMERS

The transformers are not only used to step up or step down the voltage but to control the voltage, real power and reactive power flow also. The real power is controlled by shifting the phase of the voltage and reactive power by changing the magnitude of the voltage. The voltage magnitude can be changed by changing the tap provided with the regulating transformers. There are two types of tap changers:

A) ***Off-Load Tap Changer***

Off-load tap changing needs the transformer to be de-energized. This is done to meet long-term variations, for example, growth in load, change in season, and for expanding the system.

B) ***On-Load Tap Changer/ Under Load Tap Changer***

On-load tap changing takes care of variations of system on daily, hourly or minute-by minute basis. The range of varying the tap ratio is in the range of ±10% to ±15%.

The admittance bus (Y_{BUS}) of the system modifies due to the variation of tap ratio. And thus the load flow solution also gets modified.

The on-load tap changers are treated as tap ratio in the algorithm of voltage/VAR control using PSO. It is used as a discrete variable. The tap ratios are initially generated randomly between the maximum and minimum tap ratio. The variation of taps is restricted to the existing set of tap ratios between the upper and lower limits.

4.1.2.1 *Modelling of Regulating Transformer*

Consider an ideal transformer with the transformation ratio 1: t as shown in Fig. 4.1. Y is the admittance of the transformer. It is considered on the tap-side of the transformer. I_i and I_j are the currents entering from the nodes i and j. V_i and V_j are the voltages at nodes i and j [35].

As the transformer is lossless, power flows in and out of the transformer are equal. The power flowing into the transformer, S_i is given by equation (4.2),

$$S_i = V_i I_i^* \tag{4.2}$$

The power flowing out of the transformer, S_j is given as in equation (4.3),

$$S_j = -tV_i I_j^* \tag{4.3}$$

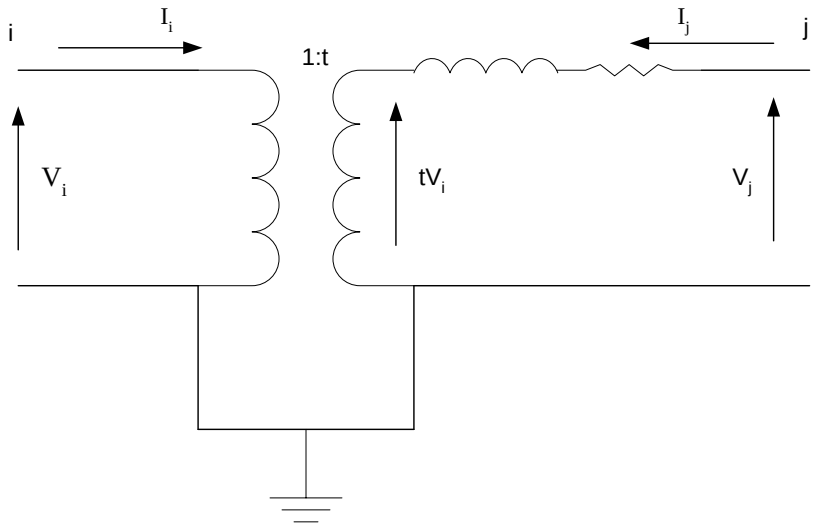

Fig. 4.1. Reactance diagram of the transformer

Equating equation (4.2) and (4.3), we have

$$I_i = -t^* I_j \tag{4.4}$$

The current I_j can be written as in equation (4.5),

$$\begin{aligned} I_j &= (V_j - tV_i)Y \\ &= -tV_iY + V_jY \end{aligned} \tag{4.5}$$

Multiply equation (4.5) by -t* and using equation (4.4)

$$I_i = tt^*YV_i - t^*YV_j \tag{4.6}$$

Put $tt^* = |t|^2$ and write equation (4.4) and (4.5) in matrix form

$$\begin{bmatrix} I_i \\ I_j \end{bmatrix} = \begin{bmatrix} |t|^2Y & -t^*Y \\ -tY & Y \end{bmatrix} \begin{bmatrix} V_i \\ V_j \end{bmatrix} \tag{4.7}$$

If t is real, equivalent π model is given as below in Fig.4.2,

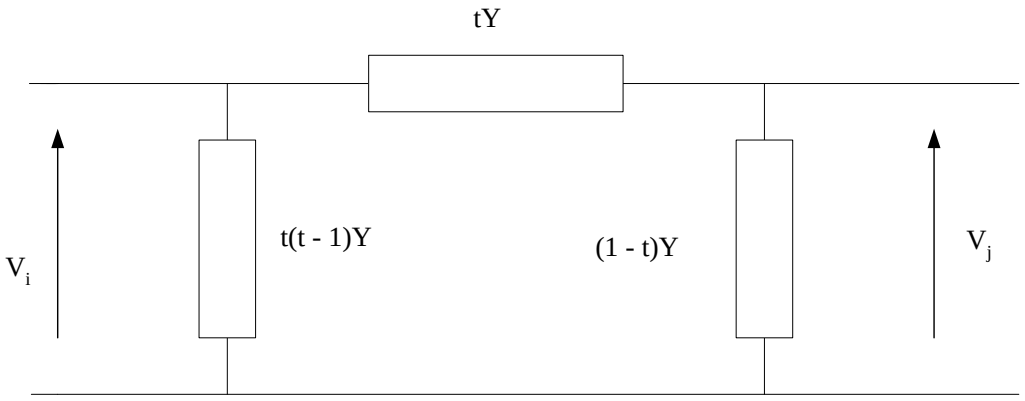

Fig. 4.2. Equivalent π model when t is real

4.1.3 SHUNT CAPACITORS

Shunt capacitors are the sources of reactive power and thus they control the voltages. The advantages of shunt capacitors are low cost, their flexibility of installation and operation. They are used to compensate for reactive losses in the transmission line.

Consider a system of an alternator supplying an inductive load as in Fig. 4.3. The phasor diagram for the same is depicted in Fig. 4.4. In this, the line current is equal to the load current.

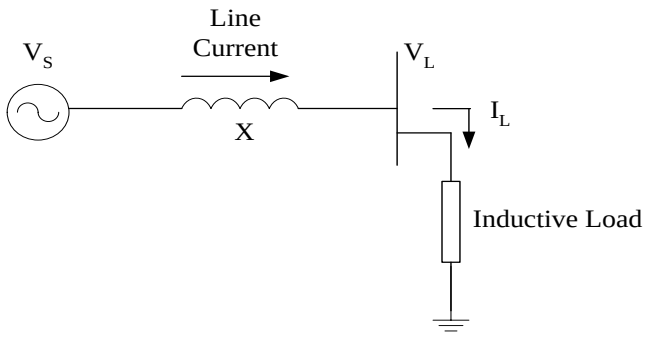

Fig. 4.3. An alternator supplying an inductive Load

.

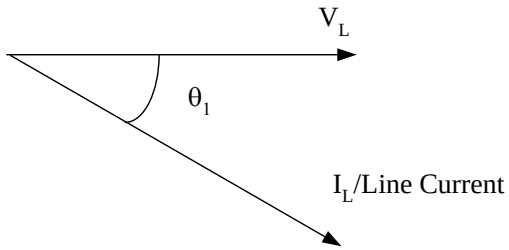

Fig. 4.4. The phasor diagram of an alternator supplying an inductive load

Now, a shunt capacitor is installed at the load bus as shown in Fig.4.5. The phasor diagram for the same is depicted in Fig.4.6.

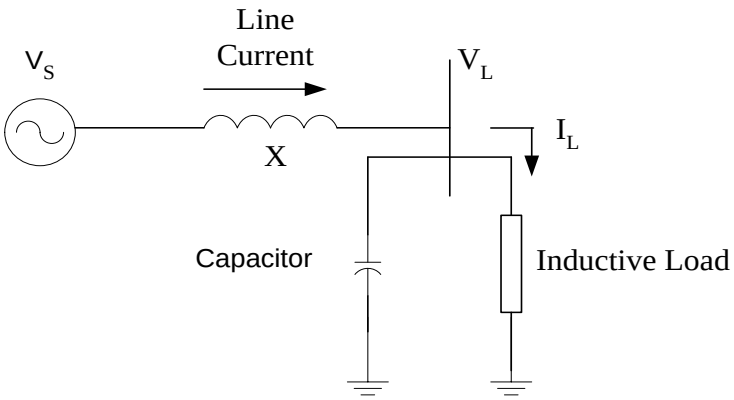

Fig. 4.5. The capacitor installed at the load bus

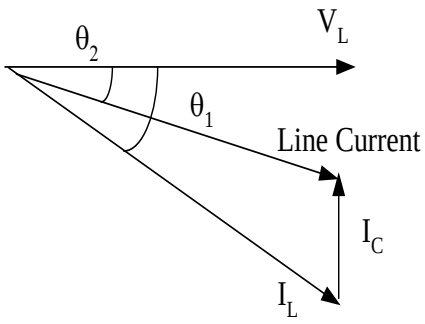

Fig. 4.6. The phasor diagram with capacitor installed

In Fig.4.6, it is shown that Θ2 is less than Θ1. Thus, it has improved the power factor. And therefore, the load will draw lesser current from the alternator and thereby I^2x losses have been reduced.

The real power consumed by the capacitor is zero and it supplies reactive power. Therefore, when it is connected at the load bus, the resultant reactive power is reduced. And hence the power factor is improved. The reactive power of capacitor is given by,

$$Q_c = \frac{V^2}{X_c} \tag{4.9}$$

Shunt capacitors are treated as no. of equipments used from the available reactive compensation equipments at the load bus in the PSO based voltage/VAR control problem. Hence it is also considered as a discrete variable. The initial values are generated randomly among the existing susceptance values and these are modified using PSO among the same set of discrete susceptance values.

The changes in the susceptance at the load bus results in change in Y_{BUS} and hence change in the load flow solution.

4.2 PROBLEM FORMULATION

The objective and constraints of the problem formulation of voltage/VAR control by minimizing the real power losses are discussed in this section.

4.2.1 OBJECTIVE

The objective of the voltage/VAR control problem is to control the voltage and VAR of the system while considering the real power loss minimization [21]. The voltage and VAR are controlled by varying automatic voltage regulator, on-load tap changer and susceptance.

$$Objective = Minimize \sum_{i=1}^{n} (P_L)_i \tag{4.10}$$

where,

n = no. of lines connected in the system

($P_{L)i}$ = real power losses in the ith branch line

subjected to the following constraints,

1) *Voltage Constraint*

If Voltage at any bus is found greater or lesser than the maximum and minimum voltage limit then a penalty is added to the solution. The penalty is added by assigning a larger value to the solution so that it becomes an inferior solution in the minimization problem and hence it gets rejected.

2) *MVA Constraint*

If MVA flow in any line in the system is obtained greater than a predetermined value then again a penalty is added to make the solution inferior. The predetermined value is taken as 1.10 times the base case MVA flow of the respective line.

Whenever the load flow solution modifies, the above constraints are checked and penalties are added.

4.2.2 ALGORITHM

Following are the steps used for the procedure of voltage/VAR control problem using different state variables discussed above:

Step1. Read bus data, branch data, generator data, base MVA, population size and no. of maximum iteration.

Step2. Find the buses whose voltages (automatic voltage regulator), susceptance values can be varied and branches whose tap ratio can be used as on-load tap changer. The minimum and maximum velocities to all the state variables are also assigned.

Step3. The Y_{BUS} and load flow is run for the base case solution. And then the MVA limit is assigned to each line.

Step4. The velocities and initial population are generated randomly within their respective limits. And for the discrete variables, population is converted to discrete.

Step5. Bus data, branch data and generator data are modified according to the population generated. And thus the Y_{BUS} and load flow solution is modified.

Step6. The objective function values are calculated using equation. (4.10) for every particle of the population.

Step7. Update the local best and global best with the consideration of objective function values. Modify the new velocities using local best, global best using equation (3.1). The state variables are also updated using equation (3.2). And for the discrete variables, population is converted to discrete.

Step8. If any violation in velocities and state variables, updated positions, they are fixed at the respective limiting values.

Step9. Compute Y_{BUS}, load flow solution for new positions, objective function value for each particle.

Step10. If iteration no. is greater than the maximum no. of iteration then stop, otherwise go to step 7.

A flowchart of PSO for voltage/VAR control problem has been depicted in Fig. 4.7.

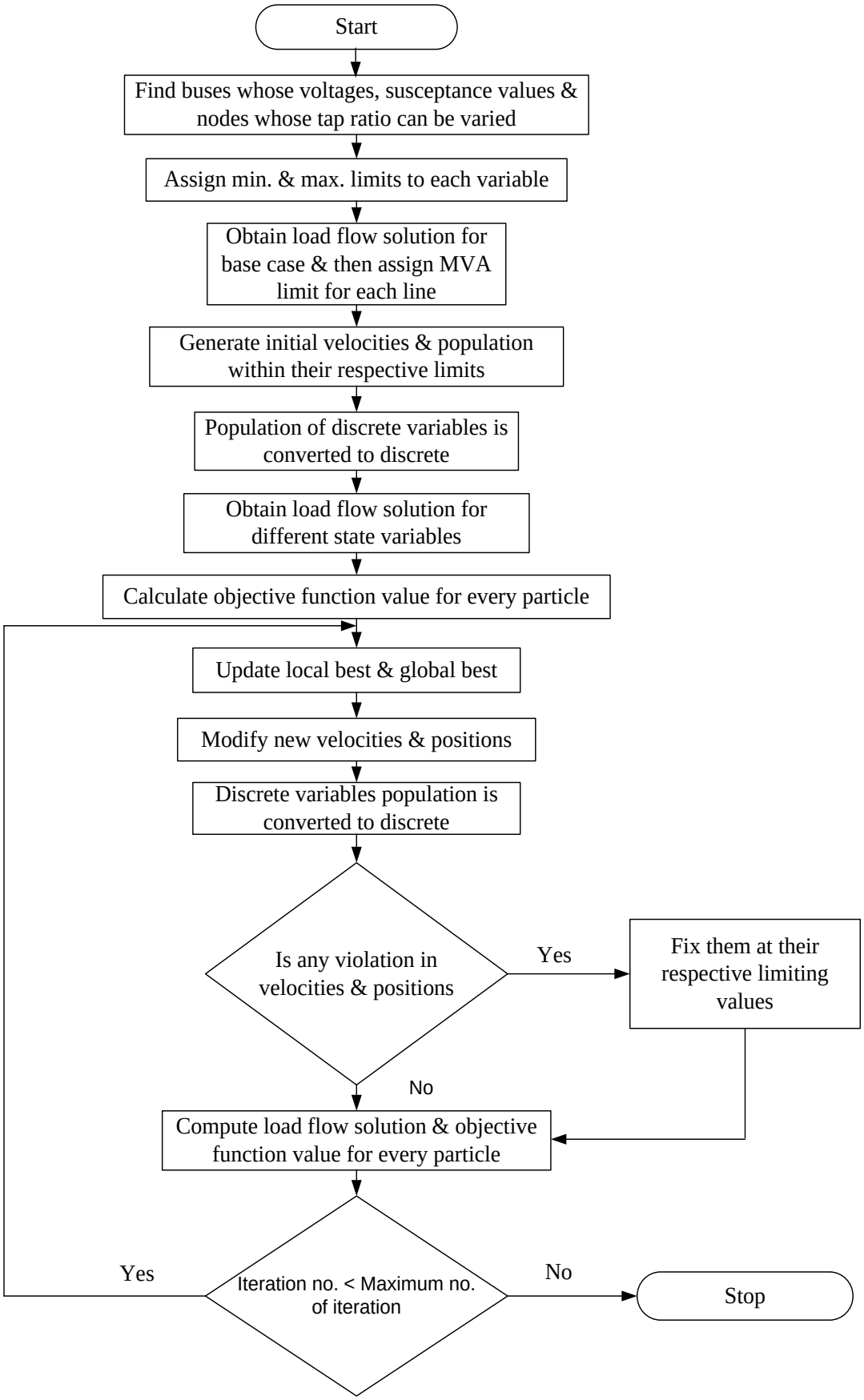

Fig. 4.7. A flowchart of particle swarm optimization for voltage/VAR control

4.3 RESULTS AND DISCUSSION

The voltage/VAR control problem using PSO has been attempted on 4-Bus, 6-Bus and 14-Bus system. The state variables used are continuous automatic voltage regulation (AVR) at PV bus, discrete tap positions (Tap) of tap-changing transformers, discrete no. of installed shunt capacitors (SC). The PSO has been used to handle both continuous and discrete variables in 14-Bus system. However, for 4-Bus and 6-Bus systems the transformer and shunt capacitor data is not available, the optimization is carried out with continuous variable i.e. PV bus voltage control using AVR.

4.3.1 CASE 1

The voltage/VAR control using PSO is carried out on 4-Bus system. It consists of one slack, one generator and two load buses. The fourth bus, P-V bus is used as continuous variable for automatic voltage regulation. The load flow analysis and line flows are summarized in Table 4.1 and 4.2 respectively for base case. The optimal control load flow analysis and line flows are given in Table 4.3 and 4.4 respectively. The loss value for the base case is 0.048091 which is minimized to 0.04787590. The minimum loss value and optimal control are given in Table 4.5.

Table 4.1. The load flow analysis for 4-Bus system (base case)

Load Flow Analysis								
Bus No.	Voltage Magnitude	Angle	Injection		Generation		Load	
	p.u.	Degree	MW	MVAR	MW	MVAR	MW	MVAR
1	1.0000	0.0000	136.809	83.511	186.809	114.501	50.000	30.990
2	0.9824	-0.9761	170.000	-105.350	0.000	0.000	170.000	105.350
3	0.9690	-1.8722	-200.000	-123.940	0.000	-0.000	200.000	123.940
4	1.0200	1.5231	238.000	131.850	318.000	181.430	80.000	49.580
Total			4.809	-13.930	504.809	295.930	500.000	309.860

Table 4.2. The line flow and losses for 4-Bus system (base case)

Line Flow and Losses							
From	To	From		To		Line Loss	
Bus	Bus	P(MW)	Q(MVAR)	P(MW)	Q(MVAR)	MW	MVAR
1	2	38.6915	22.2985	-38.4648	-31.2363	0.2267	-8.9379
1	3	98.1175	61.2124	-97.0861	-63.5687	1.0314	-2.3563
2	4	-131.5352	-74.1137	133.2507	74.9196	1.7155	0.8059
3	4	-102.9139	-60.3713	104.7493	56.9301	1.8355	-3.4412
Total Loss						4.8091	-13.9295

Table 4.3. The load flow analysis for 4-Bus system (optimal control)

Load Flow Analysis								
Bus No.	Voltage Magnitude	Angle	Injection		Generation		Load	
	p.u.	Degree	MW	MVAR	MW	MVAR	MW	MVAR
1	1.0000	0.0000	136.788	98.250	186.788	129.240	50.000	30.990
2	0.9785	-0.9320	-170.000	-105.350	0.000	-0.000	170.000	105.350
3	0.9664	-1.8476	-200.000	-123.940	0.000	0.000	200.000	123.940
4	1.0134	1.6285	238.000	117.263	318.000	166.843	80.000	49.580
Total			4.788	-13.778	504.788	296.082	500.000	309.860

Table 4.4. The line flow and losses for 4-Bus system (optimal control)

Line Flow and Losses							
From	To	From		To		Line Loss	
Bus	Bus	P(MW)	Q(MVAR)	P(MW)	Q(MVAR)	MW	MVAR
1	2	38.6325	30.1525	-38.3567	-38.8046	0.2759	-8.6521
1	3	98.1550	68.0972	-97.0529	-70.0804	1.1022	-1.9832
2	4	-131.6433	-66.5454	133.2969	67.1242	1.6536	0.5788
3	4	-102.9471	-53.8596	104.7031	50.1385	1.7559	-3.7211
Total Loss						4.7876	-13.7776

Table 4.5. The minimum loss value and optimal control for 4 Bus-system

Minimum Loss Value	
0.04787590	
State Variables	**PSO**
AVR 4	1.0134

4.3.2 CASE2

The PSO based algorithm for voltage/VAR control has also tested on 6-Bus system which has one slack, two generator and three load buses. The second and third bus voltages are taken as continuous variables. The load flow analysis and line flows for the base case are given in Table 4.6 and Table 4.8 respectively. The load flow analysis and line flows for the optimal control are summarized in Table 4.7 and Table 4.9. The minimum loss value and optimal

control values of AVR equipped buses are given in Table 4.10. The loss value is reduced from 0.078755 to 0.07713972.

Table 4.6. The load flow analysis for 6-Bus system (base case)

Load Flow Analysis								
Bus No.	Voltage Magnitude	Angle	Injection		Generation		Load	
	p.u.	Degree	MW	MVAR	MW	MVAR	MW	MVAR
1	1.0500	0.0000	107.714	35.101	107.714	35.101	0.000	0.000
2	1.0349	-3.3587	50.000	68.992	50.000	68.992	0.000	0.000
3	1.0457	-3.8233	60.000	77.368	60.000	77.368	0.000	0.000
4	0.9778	-4.0497	-70.000	-70.000	0.000	0.000	70.000	70.000
5	0.9694	-5.0731	-70.000	-70.000	-0.000	-0.000	70.000	70.000
6	0.9830	-5.6252	-70.000	-70.000	0.000	0.000	70.000	70.000
Total			7.714	-28.539	217.714	181.461	210.00	210.00

Table 4.7. The load flow analysis for 6-Bus system (optimal control)

Load Flow Analysis								
Bus No.	Voltage Magnitude	Angle	Injection		Generation		Load	
	p.u.	Degree	MW	MVAR	MW	MVAR	MW	MVAR
1	1.0500	0.0000	107.714	35.101	107.714	35.101	0.000	0.000
2	1.0349	-3.3587	50.000	68.992	50.000	68.992	0.000	0.000
3	1.0457	-3.8233	60.000	77.368	60.000	77.368	0.000	0.000
4	0.9778	-4.0497	-70.000	-70.000	0.000	0.000	70.000	70.000
5	0.9694	-5.0731	-70.000	-70.000	-0.000	-0.000	70.000	70.000
6	0.9830	-5.6252	-70.000	-70.000	0.000	0.000	70.000	70.000
Total			7.714	-28.539	217.714	181.461	210.000	210.000

Table 4.8. The line flow and losses for 6-Bus system (base case)

Line Flow and Losses							
From	To	From		To		Line Loss	
Bus	Bus	P(MW)	Q(MVAR)	P(MW)	Q(MVAR)	MW	MVAR
1	2	28.6897	-15.4187	-27.7847	12.8185	0.9049	-2.6001
1	4	43.5849	20.1201	-42.4974	-19.9326	1.0876	0.1875
1	5	35.6009	11.2547	-34.5273	13.4497	1.0735	-2.1950
2	3	2.9303	-12.2687	-2.8900	5.7281	0.0403	-6.5406
2	4	33.0909	46.0541	-31.5858	-45.1252	1.5051	0.9288
2	5	15.5145	15.3532	-15.0166	-18.0065	0.4979	-2.6534
2	6	26.2489	12.3995	-25.6656	-16.0113	0.5833	-3.6118
3	5	19.1168	23.1745	-18.0232	-26.0950	1.0936	-2.9206
3	6	43.7732	60.7242	-42.7698	-57.8610	1.0034	2.8632
4	5	4.0832	-4.9421	-4.0470	-2.7853	0.0362	-7.7274
5	6	1.6142	-9.6635	-1.5646	3.8723	0.0496	-5.7911
Total Loss						7.8755	-30.0605

Table 4.9. The line flow and losses for 6-Bus system (optimal control)

Line Flow and Losses							
From	To	From		To		Line Loss	
Bus	Bus	P(MW)	Q(MVAR)	P(MW)	Q(MVAR)	MW	MVAR
1	2	29.0070	-7.8543	-28.2148	5.0914	0.7921	-2.7628
1	4	43.3447	26.1680	-42.1276	-25.4164	1.2171	0.7515
1	5	35.3623	16.7875	-34.1619	-18.4129	1.2004	-1.6254
2	3	2.5182	-8.1733	-2.5037	1.7518	0.0144	-6.4214
2	4	33.4524	41.4271	-32.0869	-40.7230	1.3656	0.7041
2	5	15.8257	15.3182	-15.3072	-17.7845	0.5185	-2.4663
2	6	26.4185	15.3282	-25.7505	-18.5129	0.6680	-3.1847
3	5	18.7184	19.3959	-17.7965	-22.4817	0.9219	-3.0858
3	6	43.7853	56.2203	-42.8339	-53.5229	0.9514	2.6973
4	5	4.2144	-3.8606	-4.1773	-3.6484	0.0372	-7.5090
5	6	1.4429	-7.6724	-1.4156	2.0358	0.0273	-5.6366
Total Loss						7.7140	-28.5392

Table 4.10. The minimum loss value and optimal control for 6 Bus-system

Minimum Loss Value	
0.07713972	
State Variables	**PSO**
AVR 2	1.0349
AVR 3	1.0457

4.3.3 CASE 3

The PSO based algorithm is used to test IEEE-14 Bus system. The data consists of both continuous and discrete variables. Therefore, PSO is used to handle both continuous and discrete variables. The state variables used are continuous AVR equipped PV buses i.e. bus 2, 3, 6 and 8; discrete tap positions of transformers between node 4-7, 4-9 and 5-6; discrete no. of installed shunt capacitors at node 9 and 14. The load flow analysis and line flows for base case are given in Table 4.11 and Table 4.12. The load flow analysis and line flows for optimal control are summarized in Table 4.13 and Table 4.14. The minimum loss value and optimal control for 14-Bus system is tabulated in Table 4.15.

Table 4.11. The load flow analysis for 14-Bus system (base case)

Load Flow Analysis								
Bus No.	Voltage Magnitude	Angle	Injection		Generation		Load	
	p.u.	Degree	MW	MVAR	MW	MVAR	MW	MVAR
1	1.0600	0.0000	232.492	-17.144	232.492	-17.144	0.000	0.000
2	1.0450	-4.9841	18.300	29.031	40.000	41.731	21.700	12.700
3	1.0100	-12.7226	-94.200	4.938	0.000	23.938	94.200	19.000
4	1.0196	-10.3536	-47.800	3.900	0.000	0.000	47.800	-3.900
5	1.0208	-8.7864	-7.600	-1.600	-0.000	-0.000	7.600	1.600
6	1.0700	-14.1207	-11.200	-7.453	0.000	0.047	11.200	7.500
7	1.0678	-13.4384	-0.000	-0.000	-0.000	-0.000	0.000	0.000
8	1.0900	-13.4384	-0.000	13.757	-0.000	13.757	0.000	0.000
9	1.0684	-15.0213	-29.500	-16.600	-0.000	0.000	29.500	16.600
10	1.0613	-15.1505	-9.000	-5.800	-0.000	-0.000	9.000	5.800
11	1.0622	-14.7755	-3.500	-1.800	0.000	-0.000	3.500	1.800
12	1.0602	-15.0399	-6.100	-1.600	0.000	-0.000	6.100	1.600
13	1.0597	15.2923	-13.500	-5.800	-0.000	0.000	13.500	5.800
14	1.0764	-16.8527	-14.900	-5.000	0.000	-0.000	14.900	5.000
Total			13.492	-11.170	272.492	62.330	259.000	73.500

Table 4.12. The line flow and losses for 14-Bus system (base case)

Line Flow and Losses							
From	To	From		To		Line Loss	
Bus	Bus	P(MW)	Q(MVAR)	P(MW)	Q(MVAR)	MW	MVAR
1	2	156.9271	-20.4146	-152.6270	27.6941	4.3001	7.2795
1	5	75.5648	3.2708	-72.8015	2.8089	2.7633	6.0797
2	3	73.2017	3.5637	-70.8807	1.5893	2.3210	5.1530
2	4	56.2764	-2.6781	-54.5907	4.1691	1.6856	1.4910
2	5	41.4490	0.4511	-40.5501	-1.3986	0.8988	-0.9475
3	4	-23.3193	3.3489	23.6871	-3.7285	0.3677	-0.3796
4	5	-61.9883	17.6774	62.5220	-15.9932	0.5336	1.6832
4	7	28.6477	-11.8241	-28.6447	13.6720	0.0000	1.8478
4	9	16.4473	-2.3928	-16.4473	3.7806	0.000	1.3878
5	6	43.2297	12.9830	-43.2297	-8.7026	0.0000	4.2804
6	11	6.9691	0.9195	-6.9281	-0.8337	0.0410	0.0858
6	12	7.4090	0.6143	-7.3497	-0.4908	0.0593	0.1235
6	13	17.6516	-0.2841	-17.4716	0.6387	0.1801	0.3546
7	8	0.0000	-13.4769	-0.0000	13.7575	0.000	0.2806
7	9	28.6447	-0.1951	-28.6447	0.9869	0.0000	0.7917
9	10	5.6029	6.8459	-5.5811	-6.7879	0.0218	0.0579
9	14	9.9891	-7.6677	-9.8125	8.0433	0.1766	0.3756
10	11	-3.4189	0.9879	3.4281	-0.9663	0.0092	0.0216
12	13	1.2497	-1.1092	-1.2442	1.1142	0.0055	0.0050
13	14	5.2157	-7.5528	-5.0875	7.8140	0.1282	0.2611
Total Loss						13.4919	30.2328

Table 4.13. The load flow analysis for 14-Bus system (optimal control)

Load Flow Analysis								
Bus No.	Voltage Magnitude	Angle	Injection		Generation		Load	
	p.u.	Degree	MW	MVAR	MW	MVAR	MW	MVAR
1	1.0600	0.0000	232.300	-23.711	232.300	-23.711	0.000	0.000
2	1.0455	-4.9689	18.300	19.863	40.000	32.563	21.700	12.700
3	1.0144	-12.7222	-94.200	8.145	0.000	27.145	94.200	19.000
4	1.0218	-10.3239	-47.800	3.900	0.000	0.000	47.800	-3.900
5	1.0332	-8.9014	-7.600	-1.600	-0.000	0.000	7.600	1.600
6	1.0500	-14.6525	-11.200	36.493	0.000	43.993	11.200	7.500
7	1.0528	-13.5238	-0.000	-0.000	-0.000	-0.000	0.000	0.000
8	1.0500	-13.5238	-0.000	-1.689	-0.000	-1.689	0.000	0.000
9	1.0499	-15.2299	-29.500	-16.600	-0.000	0.000	29.500	16.600
10	1.0425	-15.4264	-9.000	-5.8000	-0.000	-0.000	9.000	5.800
11	1.0428	-15.1822	-3.500	-1.800	-0.000	-0.000	3.500	1.800
12	1.0372	-15.5369	-6.100	-1.600	0.000	-0.000	6.100	1.600
13	1.0345	-15.6687	-13.500	-5.800	0.000	-0.000	13.500	5.800
14	1.0346	-16.6817	-14.900	-5.000	0.000	-0.000	14.900	5.000
Total			13.300	4.802	272.300	78.302	259.00	73.500

Table 4.14. The line flow and losses for 14-Bus system (optimal control)

Line Flow and Losses							
From	To	From		To		Line Loss	
Bus	Bus	P(MW)	Q(MVAR)	P(MW)	Q(MVAR)	MW	MVAR
1	2	156.2635	-21.1916	-151.9945	28.3733	4.2690	7.1817
1	5	76.0365	-2.5196	-73.2563	8.6064	2.7802	6.0868
2	3	73.2134	1.5538	-70.9025	3.5342	2.3108	5.0880
2	4	55.9723	-3.6037	-54.3053	5.0285	1.6670	1.4248
2	5	41.1088	-6.4599	-40.2175	5.4434	0.8913	-1.0165
3	4	-23.2975	4.6111	23.6690	-4.9897	0.3715	-0.3786
4	5	-64.2600	-6.3841	64.7931	8.0659	0.5332	1.6818
4	7	29.9134	6.7248	-29.9134	-4.9897	0.0000	1.7351
4	9	17.1829	3.5205	-17.1829	-2.0103	0.000	1.5103
5	6	41.0807	-23.7156	-41.0807	29.5724	-0.0000	5.8568
6	11	5.6346	1.1432	-5.6061	-1.0836	0.0285	0.0596
6	12	7.4080	1.7418	-7.3435	-1.6075	0.0646	0.1344
6	13	16.8380	4.0353	-16.6581	-3.6811	0.1799	0.3542
7	8	0.0000	1.6932	-0.0000	-1.6887	0.0000	0.0046
7	9	29.9134	3.2964	-29.9134	-2.3976	0.0000	0.8988
9	10	6.9240	6.5952	-6.8976	-6.5251	0.0264	0.0701
9	14	10.6722	1.0521	-10.5396	-0.7699	0.1326	0.2821
10	11	-2.1024	0.7251	2.1061	-0.7164	0.0037	0.0087
12	13	1.2435	0.0075	-1.2403	-0.0046	0.0032	0.0029
13	14	4.3984	-2.1143	-4.3604	2.1918	0.0380	0.0774
Total Loss						13.2999	31.0631

Table 4.15. The minimum loss value and optimal control for 14 Bus-system

Minimum Loss Value	
0.13299914	
State Variables	**PSO**
AVR 2	1.0455
AVR 3	1.0144
AVR 6	1.05
AVR 8	1.05
Tap 4-7	0.96
Tap 4-9	0.96
Tap 5-6	1.05
SC 9	0.18
SC 14	0.06

CHAPTER-5

CONCLUSIONS AND FUTURE SCOPE OF WORK

5.1 CONCLUSIONS

The maximum loadability has been found for different load buses on different power systems using particle swarm optimization. The maximum loadability obtained from developed algorithm using PSO is compared with the respective values obtained from continuation power flow. The voltage/VAR control has also attempted using PSO by minimizing real power losses while considering both the continuous variables i.e. AVR equipped PV buses voltage, and discrete variables which are tap-settings of transformers and shunt capacitors at the load buses. The following conclusions can be drawn from the study.

- The formulation to compute maximum loadability using PSO is simple and giving the value without using any derivative method.
- The maximum loadability is close to the exact value resulted by CPF.
- The voltage/VAR control algorithm is found effective to handle both continuous and discrete variables and the constraints on MVA limit and bus voltages at load buses.

5.2 FUTURE SCOPE OF WORK

The scope of the work is identified as:

- The PSO, although giving maximum loadability close to the limit obtained by CPF. The effort can be made to obtain it as closer as possible to the limiting value by CPF .
- The voltage/VAR control of the power system can be done with the consideration of voltage security.

APPENDIX A

The data for 2-Bus [31], 4-Bus [32], 6-Bus [33] and IEEE 14-Bus test system are appended in Table A.1, A.2, A.3 and A.4 respectively. The slack, PV and load bus are denoted by 1, 2 and 3 respectively.

Table A.1 (a) Bus data 2-Bus system

Bus	Type	Voltage magnitude	Voltage Angle	Real Power Demand	Reactive Power Demand	Susceptance
1	1	1	0	0	0	0
2	3	1.004	0	100	0	0

Table A.1 (b) Generator data 2-Bus system

Bus	Real Power Generation	Reactive Power Generation	Qmax	Qmin
1	0	0	100	-100

Table A.1 (c) Branch data 2-Bus system

From Bus	To Bus	Resistance	Reactance	Line Charging Susceptance	Tap Setting
1	2	0.0	0.1	0	1

Table A.2 (a) Bus data 4-Bus system

Bus	Type	Voltage magnitude	Voltage Angle	Real Power Demand	Reactive Power Demand	Susceptance
1	1	1	0	50	30.99	0
2	3	1	0	170	105.35	0
3	3	1	0	200	123.94	0
4	2	1	0	80	49.58	0

Table A.2 (b) Generator data 4-Bus system

Bus	Real Power Generation	Reactive Power Generation	Qmax	Qmin
4	318	0	100	-100
1	0	0	100	-100

Table A.2 (c) Branch data 4-Bus system

From Bus	To Bus	Resistance	Reactance	Line Charging Susceptance	Tap Setting
1	2	0.01008	0.0504	0.1025	1
1	3	0.00744	0.0372	0.0775	1
2	4	0.00744	0.0372	0.0775	1
3	4	0.01272	0.0636	0.1275	1

Table A.3 (a) Bus data 6-Bus system

Bus	Type	Voltage magnitude	Voltage Angle	Real Power Demand	Reactive Power Demand	Susceptance
1	1	1.05	0	0	0	0
2	2	1.05	0	0	0	0
3	2	1.07	0	0	0	0
4	3	1	0	70	70	0
5	3	1	0	70	70	0
6	3	1	0	70	70	0

Table A.3 (b) Generator data 6-Bus system

Bus	Real Power Generation	Reactive Power Generation	Qmax	Qmin
1	0	0	100	-100
2	50	0	100	-100
3	60	0	100	-100

Table A.3 (c) Branch data 6-Bus system

From Bus	To Bus	Resistance	Reactance	Line Charging Susceptance	Tap Setting
1	2	0.1	0.2	0.04	1
1	4	0.05	0.2	0.04	1
1	5	0.08	0.3	0.06	1
2	3	0.05	0.25	0.06	1
2	4	0.05	0.1	0.02	1
2	5	0.1	0.3	0.04	1
2	6	0.07	0.2	0.05	1
3	5	0.12	0.26	0.05	1
3	6	0.02	0.1	0.02	1
4	5	0.2	0.4	0.08	1
5	6	0.1	0.3	0.06	1

Table A.4 (a) Bus data 14-Bus system

Bus	Type	Voltage magnitude	Voltage Angle	Real Power Demand	Reactive Power Demand	Susceptance
1	1	1.06	0	0	0	0
2	2	1.045	0	21.7	12.7	0
3	2	1.01	0	94.2	19	0
4	3	1	0	47.8	-3.9	0
5	3	1	0	7.6	1.6	0
6	2	1.07	0	11.2	7.5	0
7	3	1	0	0	0	0
8	2	1.09	0	0	0	0
9	3	1	0	29.5	16.6	19
10	3	1	0	9	5.8	0
11	3	1	0	3.5	1.8	0
12	3	1	0	6.1	2.2	0
13	3	1	0	13.5	5.8	0
14	3	1	0	14.9	5	0

Table A.4 (b) Generator data 14-Bus system

Bus	Real Power Generation	Reactive Power Generation	Qmax	Qmin
1	232.4	-16.9	10	0
2	40	42.4	50	-40
3	0	23.4	40	0
6	0	12.2	24	-6
8	0	17.4	24	-6

Table A.4 (c) Branch data 14-Bus system

From Bus	To Bus	Resistance	Reactance	Line Charging Susceptance	Tap Setting
1	2	0.01938	0.05917	0.0528	0
1	5	0.05403	0.22304	0.0492	0
2	3	0.04699	0.19797	0.0438	0
2	4	0.05811	0.17632	0.034	0
2	5	0.05695	0.17388	0.0346	0
3	4	0.06701	0.17103	0.0128	0
4	5	0.01335	0.04211	0	0
4	7	0	0.20912	0	0.978
4	9	0	0.55618	0	0.969
5	6	0	0.25202	0	0.932
6	11	0.09498	0.1989	0	0
6	12	0.12291	0.25581	0	0
6	13	0.06615	0.13027	0	0
7	8	0	0.17615	0	0
7	9	0	0.11001	0	0
9	10	0.03181	0.0845	0	0
9	14	0.12711	0.27038	0	0
10	11	0.08205	0.19207	0	0
12	13	0.22092	0.19988	0	0
13	14	0.17093	0.34802	0	0

LIST OF PUBLICATIONS

- Research paper on "A Particle Swarm Optimization for Maximum Loadability" published in International Journal of Advanced Research in Electrical, Electronics and Instrumentation Engineering, IJAREEIE, ISSN (Print): 2320-3765, ISSN(Online): 2278-8875, Vol. 2, Issue 6, June 2013.

REFERENCES

[1]	Custem T. V., "Voltage Instability: Phenomena, Countermeasures and Analysis Methods", *Proceedings of IEEE*, vol.88, pp. 208-227, 2000.
[2]	Kundur P., "Power System Stability and Control", *Mc Graw-Hill*, Power System, 1994.
[3]	Atputharajah A., Saha T.K., "Power System Blackouts-Literature Review", *International Conference on Industrial and Information Systems*, pp. 460-465, 2009.
[4]	Begovic M. M., Phadke A. G., "Control of Voltage Stability using Sensitivity Analysis", *IEEE Transactions on Power Systems*, vol.7, pp. 114-123, 1992.
[5]	Gao B., Morison G. K., Kundur P., "Voltage Stability Evaluation using Modal Analysis", *IEEE Transactions on Power Systems*, vol.7, pp. 1529-1542, 1992.
[6]	Irisarri G. D., Wang X., Tong J., Mokhtari S., "Maximum Loadability of Power Systems using Interior Point Nonlinear Optimization Method", *IEEE Transactions on Power Systems*, vol.12, pp. 162-172, 1997.
[7]	Ajjarapu V., Christy C., "The Continuation Power Flow: A Tool for Steady State Voltage Stability Analysis", *IEEE Transactions on Power Systems*, vol.7, pp. 416-423, 1992.
[8]	Chiang H., Flueck A. J., Shah K.S., Balu N., "CPFLOW: A Practical Tool for Tracing Power System Steady-State Stationary Behavior due to Load and Generation Variations", *IEEE Transactions on Power Systems*, vol.10, pp. 623-634, 1995.
[9]	Kennedy J., Eberhart R.C., "Particle Swarm Optimization", *IEEE International Conference Proceedings on Neural Networks*, vol.4, pp. 1942-1948, 1995.
[10]	Valle Y. D., Venayagamoorthy G. K., Mohagheghi S., Hernandez J. C., Harley R. G., "Particle Swarm Optimization: Basic Concepts, Variants and Applications in Power Systems", *IEEE Transactions on Evolutionary Computation*, vol.12, pp. 171-195, 2008.
[11]	Mallick S., Acharjee P., Ghoshal S. P., Thakur S. S., "Determination of Maximum Loadability using Fuzzy Logic", *International Journal of Electrical Power and Energy Systems*, vol.52, pp. 231-246, 2013.
[12]	Al Rashidi M.R., El-Harwary M.E., "A Survey of Particle Swarm Optimization Applications in Electric Power Systems", *IEEE Transactions on Evolutionary Computation*, vol.13, pp. 913-918, 2009.

[13]	Acharjee P., "Identification of Maximum Loadability Limit and Weak Buses using Security Constraint Genetic Algorithm", *International Journal of Electrical Power and Energy Systems*, vol.36, pp. 40-50, 2012.
[14]	Gnanambal K., Babulal C. K., "Maximum Loadability Limit of Power System using Hybrid Differential Evolution with Particle Swarm Optimization", *International Journal of Electrical Power and Energy Systems*, vol.43, pp. 150-155, 2012.
[15]	El-Dib A. A., Youssef H. K. M., El-Metwally M. M., Osman Z., "Maximum Loadability of Power Systems using Hybrid Particle Swarm Optimization", *Electric Power Systems Research*, vol. 76, pp. 485-492, 2006.
[16]	Arya L. D., Choube S. C., Shrivastava M., Kothari D. P., "Loadability Margin Enhancement using Co-ordinated Aggregation Based Particle Swarm Optimization", *International Journal of Electrical Power and Energy Systems*, vol.32, pp. 975-984, 2010.
[17]	Shunmugalatha A., Slochanal S. M. R., "Maximum Loadability Limit of a Power System using Multiagent-based Hybrid Particle Swarm Optimization", *Electric Power Components and Systems*, vol.36, pp. 575-586, 2008.
[18]	Shunmugalatha A., Slochanal S. M. R., "Optimum Cost of Generation for Maximum Loadability Limit of Power system using Hybrid Particle Swarm Optimization", *International Journal of Electrical Power and Energy Systems*, vol.30, pp. 486-490, 2008.
[19]	Selvi C. M., Gnanambal K., "Power System Voltage Stability Analysis using Differential Evolution", *National Conference on Innovations in Emerging Technology*, pp. 115-122, 2011.
[20]	Althowibi F. A., Mustafa M. W., "Maximum Power Systems Loadability to Detect Voltage Collapse", *4th International Power Engineering and Optimization Conference*, pp. 49-52, 2010.
[21]	Yoshida H., Kawata K., Fukuyama Y., Takayama S., Nakanishi Y., " A Particle Swarm Optimization for Reactive Power and Voltage control Considering Voltage Security Assessment" *IEEE Transactions on Power Systems*, vol.15, pp. 1232-1239, 2000.

[22]	Tomsovic K., "A Fuzzy Linear Programming Approach to the Reactive Power/ Voltage Control Problem", *IEEE Transactions on Power Systems*, vol.7, pp. 287–293, 1992.
[23]	Ramos J. L. M., Exposito A. G., Creezo J. C., Ruiz E. M., Salinas, "A Hybrid Tool to Assist the Operator in Reactive Power /Voltage Control and Optimization", *IEEE Transactions on Power Systems*, vol.10, pp. 760-768, 1995.
[24]	Cheng S. J., Malik O. P., Hope G. S., "An Expert System for Voltage and Reactive Power Control of a Power System", *IEEE Transactions on Power Systems*, vol.3, pp. 1449-1455, 1988.
[25]	Swarup K. S., Subash P. S., "Neural Network Approach to Voltage and Reactive Power Control in Power Systems", *International Conference on Intelligent Sensing and Information Processing*, pp. 228-233, 2005.
[26]	Wu X., Piao Z., Liu Y., Luo H., "Reactive Power and Voltage Control based on Improved Particle Swarm Optimization in Power System", *8th World Congress on Intelligent Control and Automation*, pp. 5291-5295, 2010.
[27]	Liu S., Zhang J., Liu Z., Wang H., "Reactive Power Optimization and Voltage Control using a Multi-objective Adaptive Particle Swarm Optimization Algorithm", *China International Conference on Electricity Distribution*, pp. 1-7, 2010.
[28]	Liang R., Wang Y., "Fuzzy-based Reactive Power and Voltage Control in a distribution System", *IEEE Transactions on Power Delivery*, vol. 18, pp. 610-618, 2003.
[29]	Vlachogiannis J. G., Lee K. Y., "Coordinated Aggregation Particle Swarm Optimization Applied in Reactive Power and Voltage Control", *IEEE Power Engineering Society General Meeting*, 2006.
[30]	Kothari D. P., Dhillon J.S., "Power System Optimization", *PHI Learning Private Limited*, 2011.
[31]	Ajjarapu V., "Computational Techniques for Voltage Stability Assessment and Control", *Springer*, 2006.
[32]	Grainger J. J., Stevenson W. D., "Power System Analysis", *Mc Graw Hill*,1994.
[33]	Wood A. J., Wollenberg B. F., "Power Generation, Operation and Control", *John Wiley and Sons*, 1996.

[34]	Kundur P., Paserba J., Ajjarapu V., Anderson G., Bose A., Canizares C., Hatziagyriou N., Hill D., Stankovic A., Taylor C. W., Cutsem T. V., Vittal V., "Definitions and Classification of Power System Stability", *IEEE/CIGRE Joint Task Force on Stability Terms and Definitions*, *IEEE Transactions on Power Systems*, vol. 19, pp. 1387-1401, 2004.
[35]	Kothari D. P., Nagrath I. J., "Power System Engineering", *Tata McGraw Hill*, 2008.